Adiponectin modulates inflammatory reactions via calreticulin receptor–dependent clearance of early apoptotic bodies

Yukihiro Takemura,[1] Noriyuki Ouchi,[1] Rei Shibata,[1] Tamar Aprahamian,[1] Michael T. Kirber,[2] Ross S. Summer,[3] Shinji Kihara,[4] and Kenneth Walsh[1]

[1]Molecular Cardiology Unit, Whitaker Cardiovascular Institute, [2]Section of Molecular Medicine, and [3]Pulmonary Center, Boston University School of Medicine, Boston, Massachusetts, USA. [4]Department of Metabolic Medicine, Graduate School of Medicine, Osaka University, Osaka, Japan.

Obesity and type 2 diabetes are associated with chronic inflammation. Adiponectin is an adipocyte-derived hormone with antidiabetic and antiinflammatory actions. Here, we demonstrate what we believe to be a previously undocumented activity of adiponectin, facilitating the uptake of early apoptotic cells by macrophages, an essential feature of immune system function. Adiponectin-deficient (APN-KO) mice were impaired in their ability to clear apoptotic thymocytes in response to dexamethasone treatment, and these animals displayed a reduced ability to clear early apoptotic cells that were injected into their intraperitoneal cavities. Conversely, adiponectin administration promoted the clearance of apoptotic cells by macrophages in both APN-KO and wild-type mice. Adiponectin overexpression also promoted apoptotic cell clearance and reduced features of autoimmunity in *lpr* mice whereas adiponectin deficiency in *lpr* mice led to a further reduction in apoptotic cell clearance, which was accompanied by exacerbated systemic inflammation. Adiponectin was capable of opsonizing apoptotic cells, and phagocytosis of cell corpses was mediated by the binding of adiponectin to calreticulin on the macrophage cell surface. We propose that adiponectin protects the organism from systemic inflammation by promoting the clearance of early apoptotic cells by macrophages through a receptor-dependent pathway involving calreticulin.

Introduction

It is becoming increasingly recognized that obesity-induced inflammation is an important component in the development of insulin-resistant diabetes and other cardiovascular disorders (1). Adiponectin (ACRP30) is an abundant circulating adipocyte-derived cytokine that is decreased in obese individuals (2–5). Epidemiological studies have implicated adiponectin in modulating insulin resistance, atherogenesis, angiogenesis, and cardiac remodeling (6–11). These effects are thought to be mediated by adiponectin binding to various cell surface receptors (12, 13) and activation of signaling pathways within the target cell (12).

Adiponectin exhibits an array of antiinflammatory properties (14, 15). Several clinical studies documented the relationship between low-plasma adiponectin concentrations and high levels of C-reactive protein, an established inflammatory marker in various populations (16–20). Experimental studies show that adiponectin reduces TNF-α production in response to various stresses in plasma, adipose tissue, vascular wall, heart, and liver (8, 9, 21–23). Adiponectin also antagonizes several of the inflammatory effects of TNF-α (15). Conversely, proinflammatory cytokines, including TNF-α, attenuate adiponectin expression in adipose tissue, resulting in a reduction of plasma adiponectin levels (15). Despite the importance of inflammation in metabolic and vascular disease, the mechanisms of immune system regulation by adiponectin are incompletely understood at a molecular level.

Adiponectin accounts for 0.01% of the total plasma protein (24). In contrast, many growth factors and cytokines that interact with cell surface receptors to activate intracellular signaling cascades are present at levels that are lower by a factor of 1,000. This led us to speculate that adiponectin has an important regulatory function that involves low-affinity macromolecular interactions. In this regard, adiponectin is structurally similar to surfactant proteins and C1q, which serve an antiinflammatory function by promoting the clearance of apoptotic cell debris. Surfactant proteins and C1q function as bridging proteins that bind to recognition motifs on dying cells and couple them to receptors on phagocytic cells (25). This activity promotes the efficient removal of apoptotic debris from the body, which is critical in preventing pathological inflammation and immune system dysfunction (26). Since obesity and hypoadiponectinemic conditions are associated with chronic inflammation (27), we tested whether adiponectin contributes to the control of systemic inflammation through an ability to promote the clearance of early apoptotic cells.

Results

To determine whether adiponectin contributes to the clearance of apoptotic particles in vivo, adiponectin-deficient (APN-KO) and WT mice were injected with dexamethasone to induce massive thymocyte apoptosis (28). At 24 hours after dexamethasone treatment, the thymi of APN-KO and WT mice were assessed for apoptotic cells in histological sections by TUNEL staining. Few TUNEL-positive cells were observed in the thymi of untreated APN-KO and WT mice. However, the thymi of dexamethasone-treated APN-KO mice showed 1.8-fold greater remnant apoptotic cells than those of similarly treated WT mice (Figure 1A); this was accompanied by a 2.7-fold increase in caspase-3 activity in tissue homogenates (data not shown). The

Nonstandard abbreviations used: Ad-APN, an adenoviral vector expressing adiponectin; Ad–β-gal, an adenoviral vector expressing β-galactosidase; ANA, anti-nuclear antibodies; APN-KO, adiponectin deficient; dsDNA, double-stranded DNA; FITC-APN, FITC-conjugated recombinant adiponectin; MALDI-MS, matrix-assisted laser desorption/ionization mass spectrometry; TAMRA, SE, 5- and 6- carboxytetramethylrhodamine, succinimidyl ester.

Conflict of interest: The authors have declared that no conflict of interest exists.

Citation for this article: *J. Clin. Invest.* **117**:375–386 (2007). doi:10.1172/JCI29709.

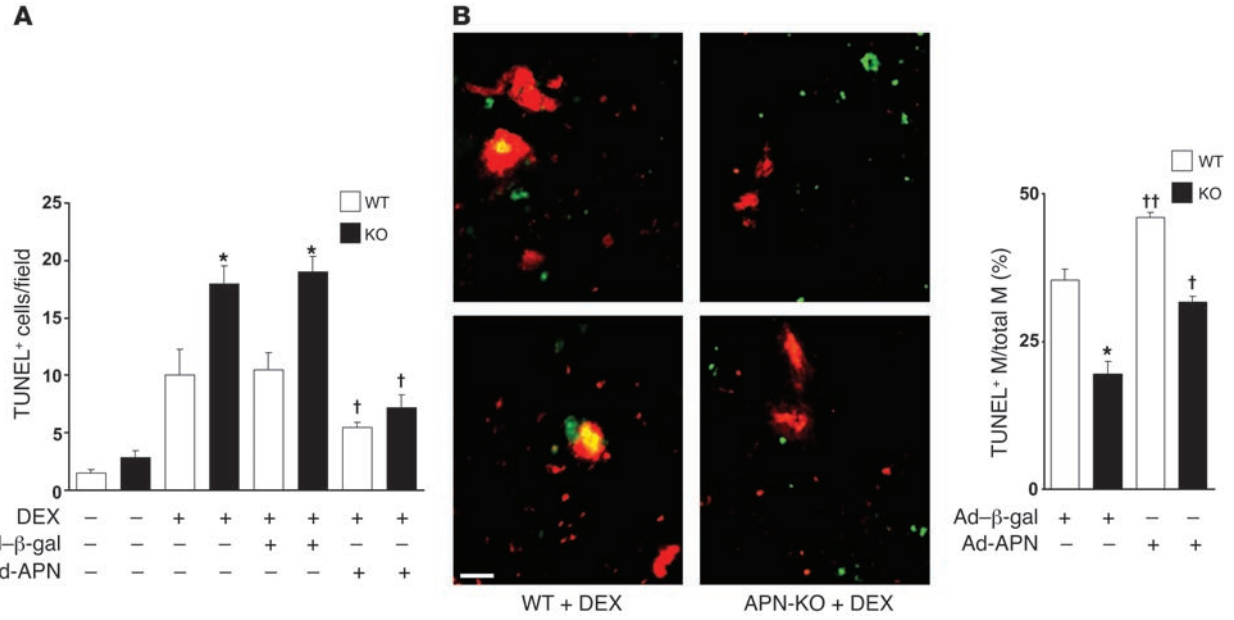

Figure 1
APN deficiency leads to the accumulation of apoptotic debris. (**A**) WT and APN-KO mice were treated with dexamethasone (DEX), and thymi were stained for apoptotic cells with TUNEL. In some experiments, mice received an i.v. infusion of Ad-APN or Ad–β-gal 2 days prior to injection of dexamethasone. The number of TUNEL-positive cells per microscopic field for the different experimental conditions is reported. *$P < 0.05$ versus WT; †$P < 0.05$ versus Ad–β-gal for WT or APN-KO ($n = 3–6$). (**B**) Adiponectin stimulates macrophage engulfment of TUNEL-positive apoptotic debris in thymi of dexamethasone-treated mice. Histological sections were stained with TUNEL (green) and anti-CD11b antibody (red). Scale bar: 20 μm. Colocalization is indicated by yellow in the merged images. ††$P < 0.01$ versus Ad–β-gal for WT or APN-KO ($n = 3–6$). M, macrophage.

i.v. preadministration of an adenoviral vector expressing adiponectin (Ad-APN) but not a control protein (Ad–β-gal) significantly diminished the level of TUNEL-positive cells in APN-KO thymi. This method of delivery results in transduction of liver, and the production of circulating adiponectin oligomers by liver is similar to that found in WT mice (11). Plasma adiponectin levels under these conditions were 13.1 ± 0.6 μg/ml in WT/Ad–β-gal, 19.0 ± 1.4 μg/ml in WT/Ad-APN, less than 0.05 μg/ml in APN-KO/Ad–β-gal, and 13.7 ± 0.5 μg/ml in APN-KO/Ad-APN. The elevation of plasma adiponectin by Ad-APN transduction in WT mice also led to a statistically significant decrease in the number of cell corpses in the thymus.

Immunohistological analysis revealed that adiponectin accumulated in the thymi of WT mice following treatment with dexamethasone (Supplemental Figure 1A; supplemental material available online with this article; doi:10.1172/JCI29709DS1), suggesting that this protein enters the damaged tissue via leakage from the vascular compartment. Thymi sections from APN-KO mice showed no signal, except in the case of Ad-APN treatment. Ad-APN–treated APN-KO mice also showed accumulation of adiponectin in the thymi of dexamethasone-treated mice. Immunofluorescent analysis of thymi sections revealed that adiponectin colocalized with the macrophage marker CD11b, suggesting that adiponectin is recruited to phagocytic cells within this tissue (Supplemental Figure 1B).

Additional histological analyses were performed on the thymi of APN-KO and WT mice that had been treated with dexamethasone to assess the percentage of macrophages containing apoptotic debris (29). The percentage of macrophages with ingested TUNEL-positive material was significantly lower in the thymi of APN-KO mice than in those of WT mice (Figure 1B). Adenovirus-mediated expression of adiponectin reversed the observed deficit in macrophage phagocytosis in APN-KO mice and increased the frequency of macrophages containing apoptotic debris in WT mice. In contrast, treatment with Ad-APN or adiponectin deficiency had no effect on the total number of macrophages present in the histological sections of thymi from either strain of mice (data not shown). To explore whether adiponectin action in the thymus could result from its ability to inhibit dexamethasone-induced apoptosis, thymocytes were isolated from WT mice and incubated with 1 μM dexamethasone in the presence or absence of recombinant adiponectin. While dexamethasone increased thymocyte apoptosis approximately 4-fold in vitro ($P < 0.05$), the inclusion of 50 μg/ml adiponectin had no detectable effect on basal or dexamethasone-induced cell death (Supplemental Figure 2). Collectively, these data suggest that the adiponectin-mediated reduction in apoptotic cells in the thymus results from the increased clearance of cell corpses rather than the inhibition of thymic cell death.

To directly determine whether adiponectin deficiency affects phagocytic activity of macrophages in vivo, early apoptotic Jurkat T cells were labeled with 5- and 6- carboxytetramethylrhodamine, succinimidyl ester (TAMRA, SE), a rhodamine fluorescent amino-reactive marker, and injected into the intraperitoneal cavity of APN-KO and WT mice (Figure 2A). These mice were pretreated with thioglycollate to recruit inflammatory macrophages, and Ad-APN or the control vector Ad–β-gal was delivered via the jugular vein of WT or APN-KO mice 3 days prior to injection of apoptotic bodies. At 30 minutes after the injection of apoptotic T cells, peritoneal cells were recovered and the uptake of apoptotic bodies was assessed by flow cytometric analysis of macrophages that were dual-labeled with F4/80, a macrophage marker, and TAMRA, SE. APN-KO mice were significantly impaired in the phagocytic uptake

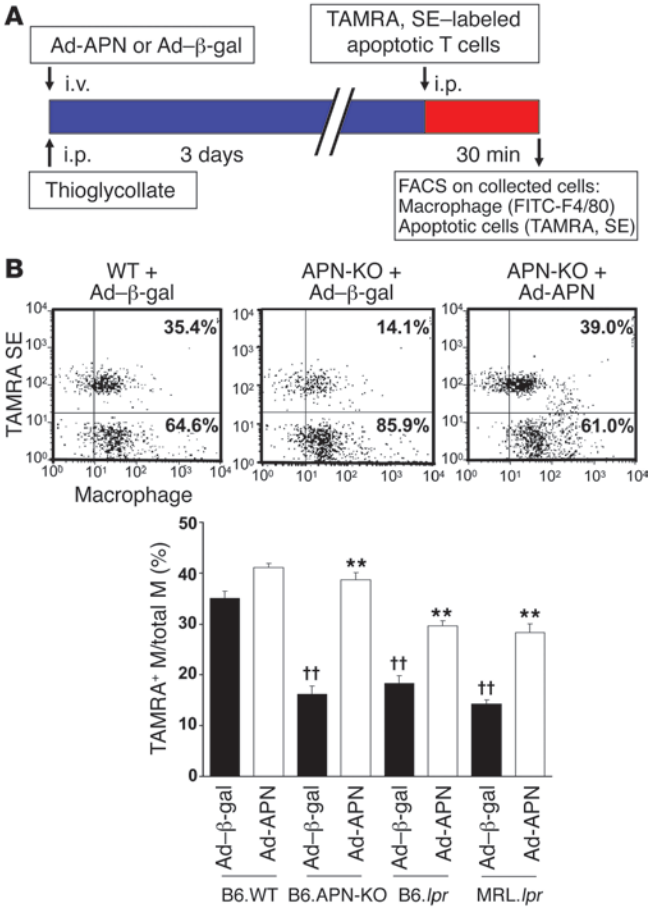

Figure 2
Systemic delivery of adiponectin promotes the uptake of apoptotic debris by peritoneal macrophages. (**A**) Strains of mice were injected with Ad–β-gal or Ad-APN on the same day as thioglycollate treatment. Circulating adiponectin levels at the time of sacrifice were 12.5 ± 1.6 μg/ml in B6.*lpr*/Ad–β-gal and 19.5 ± 2.4 μg/ml in B6.*lpr*/Ad-APN. TAMRA, SE–labeled apoptotic Jurkat T cells were injected into the peritoneum of the indicated strains of mice 3 days after the administration of thioglycollate. After 30 minutes, peritoneal cells were removed by lavage and subjected to flow cytometry. (**B**) Phagocytosis was scored as the percentage of F4/80-positive macrophages that also stained positive for TAMRA, SE. Scatter plots show representative flow cytometry data for 3 experimental conditions. Dual-labeled cells are represented in the upper right quadrant. $^{**}P < 0.01$ versus Ad–β-gal; $^{††}P < 0.01$ versus WT ($n = 6$).

of labeled apoptotic cells compared with WT mice (16.2% ± 1.6% versus 35.1% ± 1.4%, TAMRA, SE–positive macrophages, respectively) (Figure 2B). Adenovirus-mediated overexpression of adiponectin rescued the impaired apoptotic cell uptake by macrophages in the peritoneum of APN-KO mice and increased the phagocytic activity of macrophages in WT mice. Phagocytic activity could be stimulated to a similar degree if recombinant human adiponectin protein, produced in a baculovirus expression system, was injected in the intraperitoneal cavity with the apoptotic cells (Supplemental Figure 3). In these assays, adiponectin deficiency did not affect the recruitment of macrophages by thioglycollate treatment, nor did it affect peritoneal levels of TNF-α (Supplemental Figure 4).

The *lpr* mice harbor a mutation in the gene encoding Fas, and they exhibit impaired clearance of dying cells (30). This deficiency contributes to systemic inflammation and lymphadenopathy in C57BL/6 mice whereas *lpr* in the MRL/Mp$^{+/+}$ background produces more severe inflammation and animals develop autoimmune phenotypes (31, 32). Similarly to what is observed in APN-KO mice, both strains of *lpr* mice displayed an impaired clearance of apoptotic cells that were injected into the peritoneum (Figure 2A). Conversely, adenovirus-mediated overexpression of adiponectin stimulated apoptotic cell phagocytosis by macrophages in both B6.*lpr* and MRL.*lpr* mice (Figure 2B).

B6.*lpr* and MRL.*lpr* mice accumulated apoptotic debris in lymph nodes, with higher levels occurring in the MRL/Mp$^{+/+}$ background. Basal plasma adiponectin levels were 13.1 ± 0.6 μg/ml in B6.WT, 12.5 ± 1.6 μg/ml in B6.*lpr*, and 10.6 ± 0.4 μg/ml in MRL.*lpr* mice. Ad-APN administration led to plasma adiponectin levels of 19.5 ± 2.4 and 23.4 ± 3.8 μg/ml in B6.*lpr* and MRL.*lpr* mice, respectively, at 3 days after infection and decreased levels of TUNEL-positive material in submandibular lymph nodes of both strains relative to those of control mice that were treated with the equivalent titer of Ad–β-gal (Figure 3A). Both B6.*lpr* and MRL.*lpr* mice developed autoreactive anti-nuclear antibodies (ANA), although levels were higher in the MRL background. Fourteen days after Ad-APN treatment, ANA levels were reduced by factors of 8.9 and 3.6 in B6.*lpr* and MRL.*lpr* mice, respectively (Figure 3B). ANA levels were not detectable in WT mice (data not shown). MRL.*lpr* but not B6.*lpr* mice also develop anti–double-stranded DNA (anti-dsDNA) antibodies, which are found in patients with systemic lupus erythematosus. Adiponectin overexpression lowered the mean level of anti-dsDNA antibodies by a factor of 4.6 in MRL.*lpr* mice. The effects of adiponectin overexpression on renal function and morphology were also evaluated because this organ is damaged by the autoimmune disease in MRL.*lpr* mice. Adiponectin overexpression led to a modest but reproducible reduction in glomerular tuft volume at 14 days following Ad-APN delivery (Figure 3C) and reduced the accumulation of immune complex deposition in the kidney as assessed by immunofluorescence (data not shown). Consistent with these findings, adiponectin overexpression suppressed urinary albumin excretion (Figure 3C). Additional studies showed that MRL.*lpr* mice displayed normal glucose sensitivity relative to MRL/Mp$^{+/+}$ mice and that adenovirus-mediated overexpression of adiponectin in MRL.*lpr* mice did not affect body weight or circulating insulin levels (Supplemental Figure 5, A–C). Thus, adiponectin's actions in this model were largely antiinflammatory rather than metabolic. Consistent with this notion, adiponectin overexpression led to a reduction in circulating TNF-α in MRL.*lpr* mice (Supplemental Figure 5D).

APN-KO/*lpr* mice were generated on the C57BL/6 background so that we could evaluate whether adiponectin deficiency would further impair apoptotic cell clearance and promote inflammation relative to the B6.*lpr* and APN-KO parental strains. Macrophage uptake of apoptotic cells in the peritoneum of APN-KO/*lpr* mice was significantly less than in either parental strain as assessed by flow cytometric analysis of TAMRA, SE and F4/80 dual-positive macrophages at 10 weeks of age (Figure 4A). At this age, plasma levels of TNF-α are similar between APN-KO, *lpr*, and APN-KO/*lpr* strains, but by 20 weeks of age, APN-KO/*lpr* mice display much higher levels of TNF-α than the other strains (Supplemental Figure 6). B6.*lpr* mice develop age-dependent lymphadenopathy and autoimmunity starting at approximately 10 weeks of age (32, 33). Lymphadenopathy was markedly increased in APN-KO/*lpr* compared with *lpr* mice

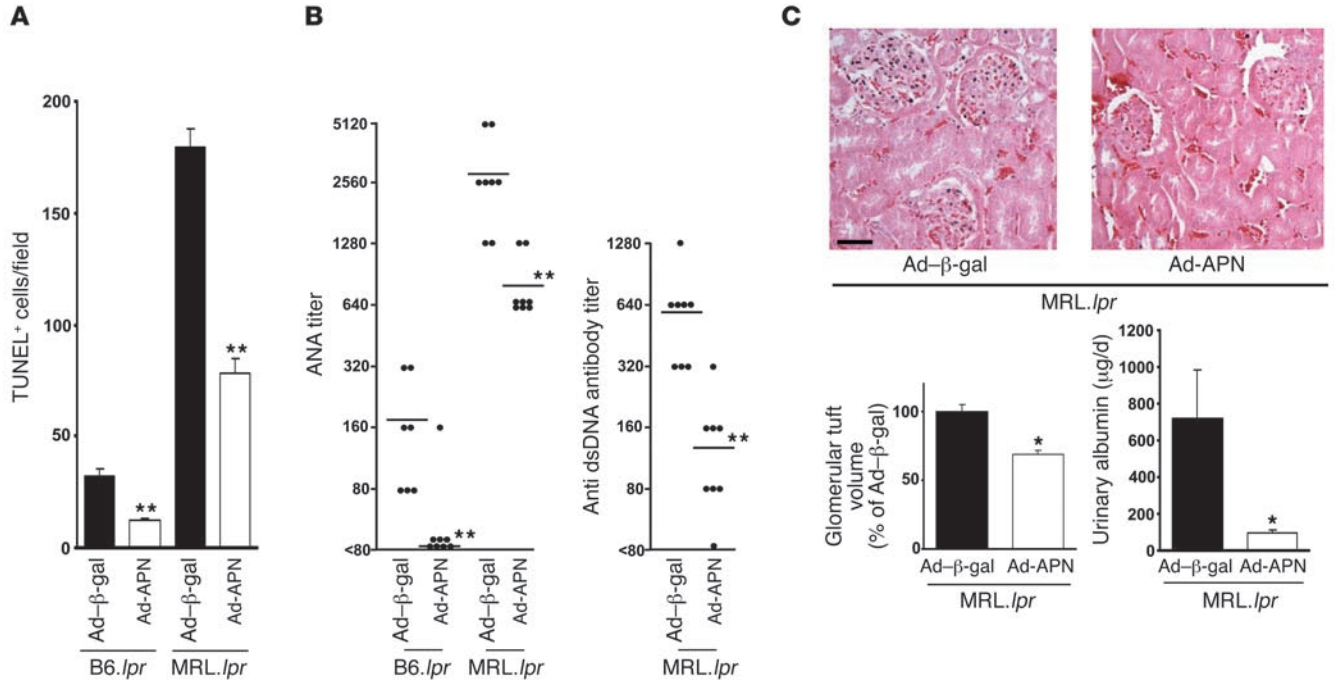

Figure 3

Systemic delivery of adiponectin decreases remnant apoptotic levels and inflammation in *lpr* strains of mice. (**A**) Adenovirus-mediated overexpression of adiponectin decreases apoptotic cells in lymph nodes of B6.*lpr* mice at the age of 12 weeks and MRL.*lpr* mice at the age of 20 weeks. Lymph node sections were stained with TUNEL and quantified by microscopy (n = 6–8). (**B**) ANA titers and anti-dsDNA antibody titer in the serum of B6.*lpr* or MRL.*lpr* mice at 14 days after Ad-APN or Ad–β-gal administration. $^{**}P < 0.01$ versus Ad–β-gal. (**C**) Adiponectin overexpression influences renal function and morphology. Photographs show representative glomeruli of MRL.*lpr* mice treated with Ad–β-gal or Ad-APN 14 days prior to sacrifice. Glomerular tuft volume of control is $3.1 \times 10^5 \pm 0.1 \times 10^5$ μm^3. Scale bar: 50 μm. Urinary albumin is reported as μg protein/d. $^{*}P < 0.05$ versus Ad–β-gal (n = 8).

at 20 weeks of age, and a statistically significant increase in submandibular lymph node size could be detected in the APN-KO/*lpr* strain as early as 12 weeks of age (Figure 4B). The lymph nodes from APN-KO/*lpr* mice displayed higher levels of TUNEL-positive cells compared with those of *lpr* mice at both 12 and 20 weeks of age whereas the lymph nodes of APN-KO and WT mice showed few or no TUNEL-positive cells (Figure 4C). Adiponectin deficiency also produced an increase in ANA titers by 2.7- and 4.1-fold in *lpr* mice at 12 and 20 weeks of age, respectively (Figure 4D). Furthermore, adiponectin deficiency led to detectable anti-dsDNA antibody titers in *lpr* mice at 20 weeks of age whereas the parental B6.*lpr* strain showed little or no dsDNA immunoreactive material. No anti-dsDNA antibodies could be detected at 12 weeks of age. Both APN-KO and WT mice showed no evidence of autoreactive antibodies (Figure 4D). Finally, the APN-KO/*lpr* mice displayed features of kidney dysfunction associated with autoimmune disease, including glomerular tuft enlargement and proteinuria, whereas WT, APN-KO, and *lpr* mice in the C57BL/6 background did not (Figure 4E). These data show that adiponectin deficiency in B6.*lpr* mice leads to further reductions in apoptotic cell clearance and exacerbates systemic inflammation. Furthermore, these data show that a detectable impairment in apoptotic cell clearance coincides with or precedes the development of the autoimmune and lymphoproliferative phenotypes.

To investigate the mechanism by which adiponectin affects early apoptotic body clearance in vitro, FITC-labeled macrophages from different sources were incubated with viable or apoptotic Jurkat T cells labeled with TAMRA, SE in the presence or absence of adiponectin. Recombinant human adiponectin, produced from a baculovirus expression system, stimulated the uptake of apoptotic Jurkat T cells by 32.8% ± 1.0% by human monocyte-derived macrophages and 23.6% ± 0.4% in differentiated monocytic THP-1 cells in vitro, as determined by flow cytometric analysis of dual-labeled and total macrophages (Figure 5). In agreement with these data, microscopic analyses also revealed that adiponectin stimulated the ingestion of TAMRA, SE–labeled apoptotic cells by human and THP-1 macrophages (Supplemental Figure 7). Recombinant adiponectin was either equally effective or more effective at promoting phagocytosis than C1q (Figure 5), which promotes apoptotic cell uptake by macrophages and is implicated in the development of autoimmune disease (34, 35). Stimulation of apoptotic cell uptake was dependent on the dose of adiponectin in the phagocytosis assay, and this effect appeared to saturate at a final concentration of 4 μg/ml adiponectin (Supplemental Figure 8). Recombinant adiponectin also stimulated the uptake of early apoptotic neutrophils by THP-1 and human macrophages (Supplemental Figure 9A) but had no effect on the uptake of microbeads opsonized with BSA, IgG, or C3b (Supplemental Figure 9B). Adiponectin did not stimulate the uptake of viable Jurkat T cells by human or THP-1 macrophages (Supplemental Figure 9C). Furthermore, adiponectin did not stimulate the uptake of late apoptotic bodies by human or THP-1 macrophages (Supplemental Figure 9D).

To determine whether adiponectin promotes phagocytosis through an opsonization mechanism, we examined the binding of adiponectin to early apoptotic and viable Jurkat T cells using stan-

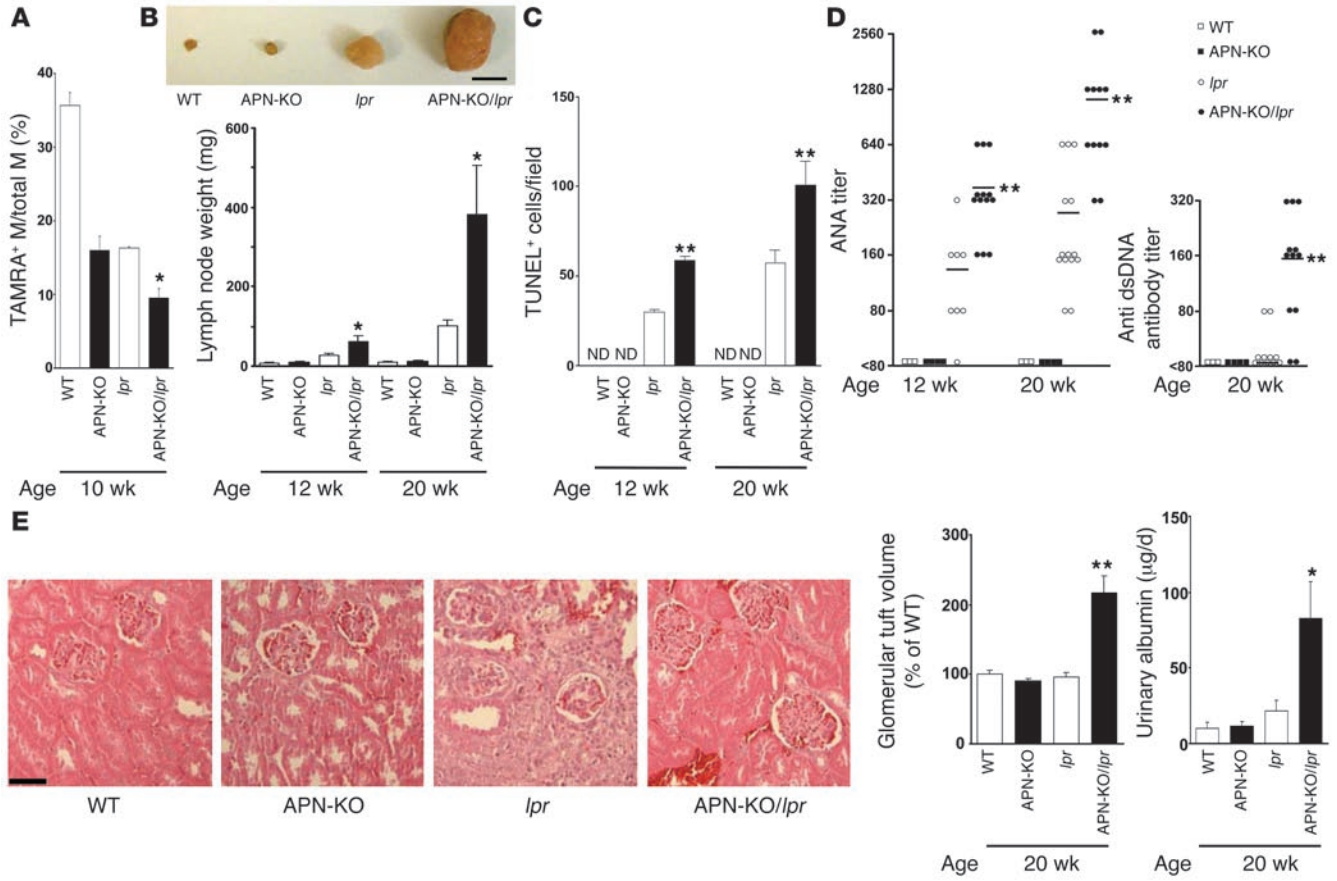

Figure 4

B6/*lpr* mice deficient in adiponectin display impaired clearance of apoptotic cells and increased systemic inflammation. (**A**) Impaired clearance of apoptotic cells by peritoneal macrophages in APN-KO/*lpr* mice compared with APN-KO and *lpr* mice. Experiments were conducted with the indicated strains of mice. Phagocytosis of apoptotic Jurkat cells was assessed by flow cytometric analysis of F4/80- and TAMRA, SE–positive cells as described in the Figure 1C legend. **P* < 0.05 versus B6/*lpr* APN-KO (*n* = 4–6). (**B**) APN-KO/*lpr* mice have larger submandibular lymph nodes compared with *lpr* mice. Inset shows a representative photograph of submandibular lymph nodes from each strain of mouse at the age of 20 weeks. Scale bar: 5 mm. Submandibular lymph nodes were excised from the indicated strains of mice at 12 or 20 weeks and weighed. **P* < 0.05 versus *lpr* (*n* = 6–14). (**C**) Adiponectin deficiency increases the frequency of apoptotic cells in lymph nodes of B6.*lpr* mice. Mice were sacrificed at 12 or 20 weeks of age, and TUNEL-positive cells in sections of submandibular lymph nodes were assessed. ND, not detectable. ***P* < 0.01 versus *lpr* (*n* = 6–14). (**D**) Adiponectin deficiency increases autoreactive antibody titer in B6.*lpr* mice. ANA titers and anti-dsDNA antibody titers in the sera of each strain of mouse were determined at 12 or 20 weeks of age. ***P* < 0.01 versus *lpr* (*n* = 3–14). (**E**) Adiponectin deficiency promotes kidney disease in B6.*lpr* mice. Glomerular tuft volume was determined in histological sections of kidney from the indicated strains of 20-week-old mice. Photographs show representative glomeruli. The calculated glomerular tuft volume of control is $1.1 \times 10^5 \pm 0.1 \times 10^5$ μm^3. Scale bar: 50 μm. ***P* < 0.01 versus *lpr*. The daily excretion of urinary albumin was determined immediately prior to sacrifice. **P* < 0.05 versus *lpr* (*n* = 4–10).

dard protocols (25, 35). Cells were incubated with FITC-conjugated recombinant human FITC-APN for 60 minutes. Fluorescence microscopy revealed that adiponectin bound to blebs on Jurkat T cells that were morphologically apoptotic following exposure to UVB irradiation with a high, locally intense signal (Figure 6A). Adiponectin also bound to viable Jurkat T cells, but the fluorescence intensity was weak and more uniformly distributed on the cell surface. Flow cytometry was performed to quantify adiponectin binding to viable and apoptotic Jurkat cells (Figure 6B). This analysis revealed greater binding of adiponectin to apoptotic cells compared with viable cells. These findings were corroborated by analyzing adiponectin binding to viable and apoptotic cells using a microplate reader and FITC-labeled adiponectin (Supplemental Figure 10A). More adiponectin was bound to apoptotic cells than viable cells over a wide range of adiponectin concentrations. Collectively, these data show that the expression of an adiponectin receptor is upregulated on the cell surface of the dying cell.

To investigate the mechanism by which adiponectin modulates the clearance of apoptotic cells, detergent-solubilized membrane fractions from THP-1 macrophages were incubated with or without polyhistidine-tagged adiponectin protein, precipitated with nickel resin, and subjected to SDS-PAGE. One unique protein band was detected when membrane fractions were treated with nickel resin in the presence of adiponectin but not in its absence (data not shown). This region of SDS-PAGE gel was excised, treated with trypsin, and analyzed by matrix-assisted laser desorption/ionization mass spectrometry (MALDI-MS). Peptide mass fingerprints were analyzed with the protein prospector program MS-Fit (University of California, San Francisco, Mass Spectrometry Facility: http://prospector.ucsf.edu/prospector) using the database

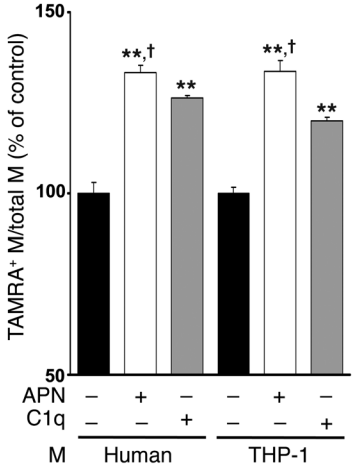

Figure 5
Adiponectin promotes the phagocytosis of apoptotic bodies by macrophages in vitro. Apoptotic Jurkat T cells were preincubated for 1 hour with recombinant adiponectin from baculovirus-insect (APN) (50 μg/ml), human C1q (50 μg/ml), or vehicle. Macrophages were then incubated for 30 minutes with TAMRA, SE–labeled Jurkat cells that were either viable or apoptotic due to UVB exposure. Upon mixing apoptotic cells with macrophages, adiponectin and C1q were diluted to a final concentration of 10 μg/ml. Phagocytosis was assessed by flow cytometry. Macrophages were stained with FITC-conjugated anti-human macrophage antibody, and the percentage of phagocytic macrophages was calculated as TAMRA, SE–positive (+) macrophages/total macrophages × 100%. Phagocytic macrophages of control were 32.8% ± 1.0% (human) and 23.6% ± 0.4% (THP-1). $^{**}P < 0.01$ versus vehicle; $^{\dagger}P < 0.05$ versus C1q (n = 6–7).

NCBInr.2005.01.06, and 13 peptide masses were found to correspond to calreticulin and cover 33% of the protein sequence. To confirm the presence of calreticulin in the nickel resin precipitate, Western immunoblot analysis was performed with anti-calreticulin antibody. Calreticulin was only detected in the THP-1 membrane fraction when the precipitation with nickel resin was performed in the presence of polyhistidine-tagged adiponectin (Figure 7A). Adiponectin binding to calreticulin was also demonstrated by immunoprecipitating the solubilized THP-1 membrane fraction with anti-calreticulin antibodies followed by the detection of adiponectin by Western immunoblot analysis (Figure 7B). To determine whether adiponectin binds to calreticulin on the cell surface, competition assays between recombinant adiponectin and anti-calreticulin antibody were performed using intact THP-1 macrophages (35). Preincubation with adiponectin for 60 minutes significantly reduced the binding of anti-calreticulin antibody to THP-1 macrophages as determined by flow cytometric analysis of FITC-conjugated secondary antibody to the anti-calreticulin antibody (Figure 7C).

Recent studies have shown that calreticulin is upregulated on the surface of the apoptotic cell, where it acts as a general recognition ligand in the phagocytic process (36). Accordingly, more calreticulin could be detected on apoptotic Jurkat T cells than viable cells by flow cytometric analysis (Supplemental Figure 10B). Preincubation with anti-calreticulin antibody partially but significantly inhibited the binding of adiponectin to apoptotic cells (Supplemental Figure 10C). Finally, adiponectin could be colocalized with calreticulin on apoptotic thymic cells in mice that were treated with dexamethasone (Supplemental Figure 10D).

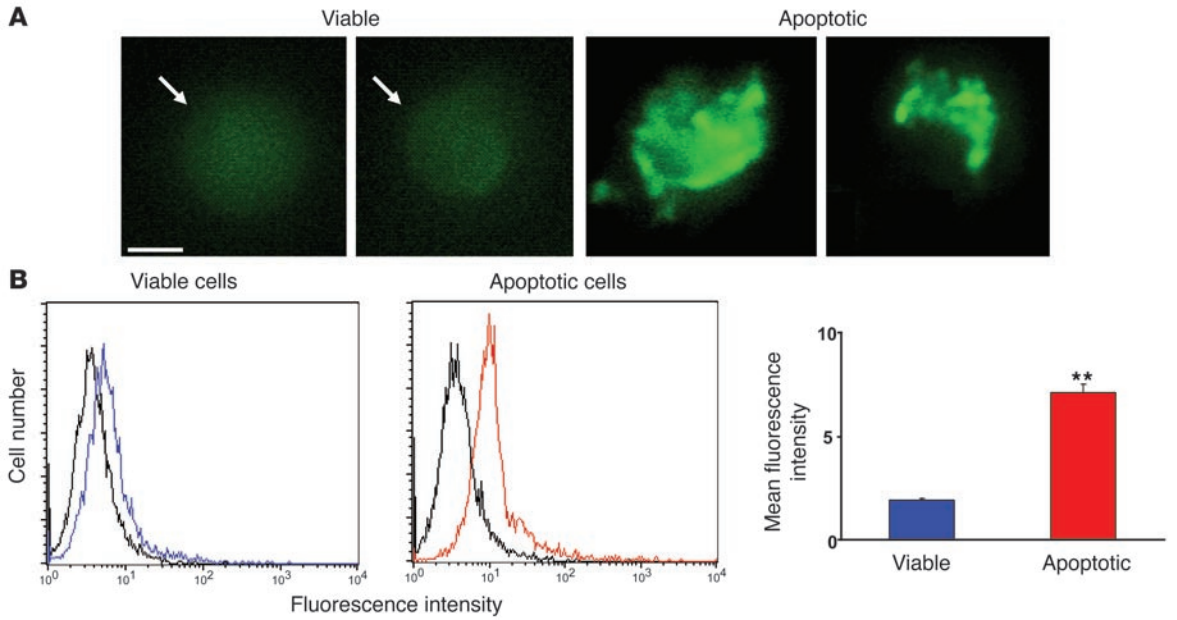

Figure 6
Apoptosis increases the binding of adiponectin to Jurkat T cells. (**A**) Fluorescence microscopy of FITC-APN to viable (left panel) and apoptotic (right panel) Jurkat T cells. Binding to viable cells was diffuse whereas binding to apoptotic cells was intense and uneven within individual cells. Scale bar: 5 μm. (**B**) Left panels: representative flow cytometric analyses of FITC-APN to viable (blue) and apoptotic Jurkat T (red) cells. Control (black) represents cells incubated with FITC-conjugated human serum albumin. Right panel: Quantitation of FITC-APN binding to viable and apoptotic cells. $^{**}P < 0.01$ versus viable cells (n = 3).

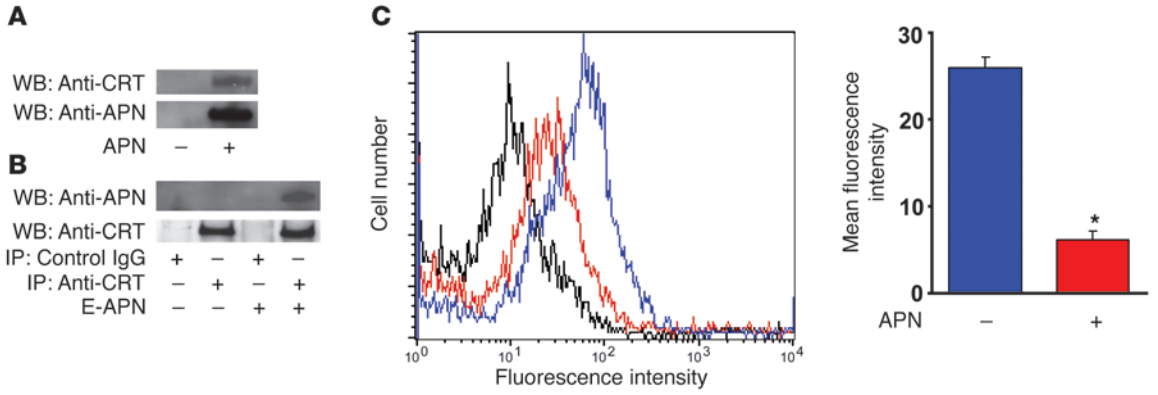

Figure 7

Adiponectin interacts with calreticulin on the macrophage cell surface. (**A**) Calreticulin is immunoprecipitated by histidine-tagged adiponectin (APN) from detergent-solubilized THP-1 membranes. Membrane fractions were incubated in the presence or absence of polyhistidine-APN and then precipitated with nickel resin. The resin was then treated with a molar excess of histidine to release precipitated proteins, and this material was subjected to SDS-PAGE followed by immunoblot analysis with anti-calreticulin (anti-CRT) and anti-adiponectin (anti-APN) antibodies. WB, Western blot. (**B**) Adiponectin prepared from *E. coli* (E-APN) was immunoprecipitated from detergent-solubilized THP-1 membranes by anti-calreticulin antibodies. THP-1 membrane fractions were incubated in the presence or absence of polyhistidine APN and then subjected to immunoprecipitation with anti-CRT or control IgG. Immunoprecipitated material was then subjected to SDS-PAGE, and Western blot analysis was performed with anti-APN or anti-CRT antibodies. (**C**) Adiponectin inhibits the binding of anti-calreticulin antibody to macrophages. THP-1 macrophages were preincubated with 200 μg/ml adiponectin (red) or vehicle (blue) for 60 minutes followed by incubation with anti-calreticulin antibody (10 μg/ml) for 60 minutes. Cells incubated with chicken IgY followed by treatment with FITC-conjugated secondary antibody served as control. Cells were then incubated with FITC-conjugated secondary antibody to anti-calreticulin antibody and analyzed by flow cytometry. *$P < 0.05$ versus vehicle ($n = 3$).

The binding of FITC-labeled adiponectin to the phagocytic cell surface was also analyzed. Recombinant human adiponectin binding to THP-1 macrophages was saturable, with half-maximal binding occurring at approximately 0.7 μg FITC-APN/ml (Supplemental Figure 11A). Coincubation with 6 μg/ml FITC-APN and anti-calreticulin antibody led to a 37.1% ± 7.2% ($P < 0.05$) reduction in APN binding compared with control antibody (Supplemental Figure 11B), suggesting that adiponectin interacts with calreticulin in addition to other adiponectin receptors, such as AdipoR1, AdipoR2, and T-cadherin, on the macrophage cell surface. Finally, adiponectin colocalized with calreticulin on the surface of THP-1 cells (Supplemental Figure 11C).

To determine whether adiponectin increases macrophage-mediated removal of early apoptotic bodies through a calreticulin-dependent pathway in vitro, macrophages from different sources were incubated with recombinant adiponectin or vehicle in the presence or absence of anti-calreticulin antibody, and the uptake of apoptotic Jurkat T cells was assessed by flow cytometry (Figure 8A). Preincubation with anti-calreticulin antibody blocked adiponectin-stimulated phagocytosis of apoptotic bodies. This treatment had no effect on basal phagocytosis in human macrophages or THP-1 cells, consistent with a previous report (25). Calreticulin interacts with endocytic receptor protein CD91 to phagocytose apoptotic cells (35). Accordingly, adiponectin-mediated uptake of apoptotic cells was also blocked by incubation with anti-CD91 antibody. To corroborate these data, knockdown experiments were performed with siRNA targeting calreticulin and CD91. Calreticulin expression was reduced by 60.6% ± 2.5%, and CD91 expression was reduced by 92.6% ± 1.8% by treatment with their corresponding siRNA polynucleotides (Supplemental Figure 12), leading to 68% and 95% reductions, respectively, in adiponectin-stimulated apoptotic cell uptake by THP-1 macrophages (Figure 8B).

AdipoR1, AdipoR2, and T-cadherin are also reported to function as adiponectin receptors (12, 13). To assess whether these receptors are associated with the removal of apoptotic debris by adiponectin, AdipoR1, AdipoR2, and T-cadherin expression was knocked down by RNA interference methods. AdipoR1 was reduced by 69.5% ± 6.1%, AdipoR2 was reduced by 51.6% ± 5.0%, and T-cadherin was reduced by 74.1% ± 11.7%, as determined by flow cytometric analysis of cell-surface protein expression (Supplemental Figure 12). However, reductions of AdipoR1, AdipoR2, or T-cadherin had no influence on adiponectin-stimulated phagocytosis (Figure 8B). Collectively, these data suggest that adiponectin can increase the removal of apoptotic bodies via calreticulin/CD91 but not through the previously identified adiponectin receptors.

Discussion

The present study demonstrates that adiponectin can facilitate the removal of early apoptotic cells by macrophages and modulate the processes of inflammation and autoimmunity. Excess adiposity is associated with immune system dysfunction and inflammation in both humans and mouse models of obesity (27). Adipose tissue produces a variety of proinflammatory substances, including leptin, IL-6, TNF-α, and complement factors. Most of these factors are positively associated with adiposity, and they promote inflammation. In contrast, adiponectin is downregulated in obesity-linked disease, and it participates in limiting inflammatory reactions (15). Clinically, plasma adiponectin levels inversely correlate with levels of C-reactive protein in humans (16, 20). Experimental studies with mice showed that adiponectin deficiency results in increased inflammation under conditions of overnutrition or tissue ischemia (8, 21). These antiinflammatory effects are mediated, at least in part, by the ability of adiponectin to inhibit LPS-stimu-

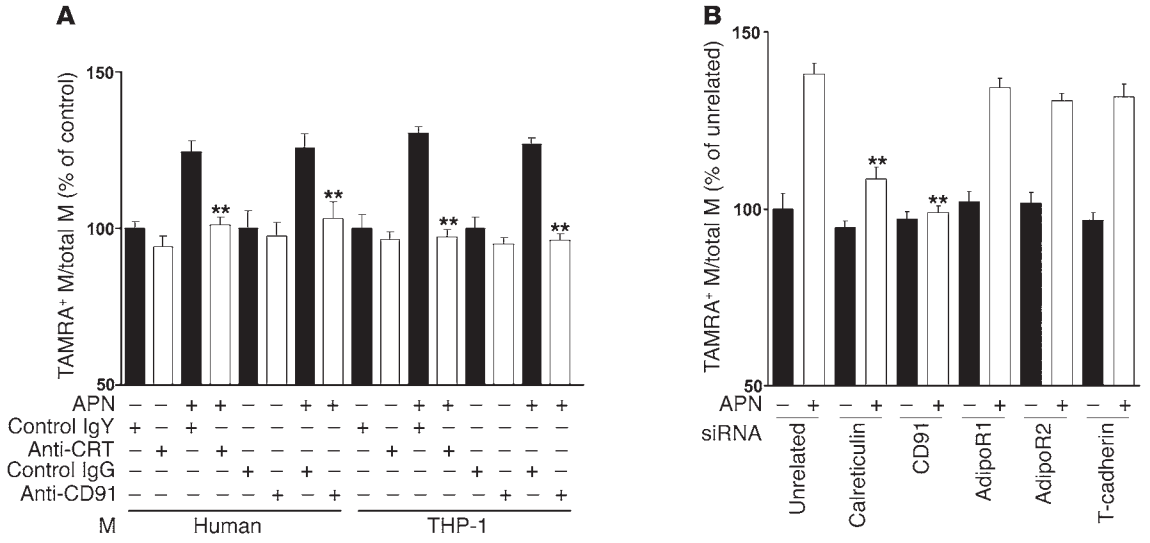

Figure 8

Calreticulin and CD91 are essential for adiponectin-stimulated uptake of apoptotic cells. (**A**) Anti-calreticulin antibody and anti-CD91 antibody inhibit adiponectin-stimulated apoptotic cell phagocytosis by macrophages. Each type of macrophage was preincubated with anti-CRT antibody or control chicken IgY or with anti-CD91 antibody or control IgG for 60 minutes. TAMRA, SE–labeled apoptotic cells were preincubated with recombinant adiponectin or vehicle, and uptake of apoptotic debris was determined by flow cytometric analysis. Data are expressed relative to control from human and THP-1 monocytes. Control human and THP-1 macrophages (anti-human macrophage antibody-positive) were 34.1% ± 0.8% and 24.9% ± 1.1% dual-positive for TAMRA, SE, respectively. $^{**}P < 0.01$ versus IgY or IgG (n = 6–7). (**B**) Adiponectin-stimulated apoptotic cell phagocytosis by macrophages was inhibited by downregulation of calreticulin or CD91 with siRNA but not siRNA targeting the putative adiponectin receptors. The in vitro phagocytosis assay analyzed dual-positive by cells flow cytometry. Control THP-1 macrophages were 24.3% ± 1.0% positive for TAMRA, SE. $^{**}P < 0.01$ versus unrelated siRNA with adiponectin (n = 6–7).

lated TNF-α production and increase antiinflammatory cytokine IL-10 expression in macrophages (15, 37, 38).

The findings reported here suggest that facilitation of early apoptotic body phagocytosis is an additional mechanism by which adiponectin limits inflammatory responses. Failure to rapidly clear dying cells by macrophages will promote inflammation either by allowing late apoptotic cells to undergo secondary necrosis and release noxious substances to the tissues or by the presentation of these corpses to follicular dendritic cells, leading to T cell activation (26). It has also been reported that the uptake of late apoptotic cells by macrophages will promote the secretion of proinflammatory cytokines (39). These processes can lead to systemic inflammation and, under extreme conditions, breach self tolerance, contributing to autoimmune disease. Conversely, it is well recognized that the uptake of early apoptotic debris can, under some circumstances, have an immunosuppressive effect on the cell that is associated with the downregulation of TNF-α and the upregulation of IL-10 (40–42).

Multiple lines of evidence show that physiological levels of adiponectin promote the clearance of early apoptotic cells. Baculovirus-produced human adiponectin stimulated the in vitro uptake of labeled apoptotic cells by both human and THP-1 macrophages as assessed by flow cytometric analysis of dual-positive anti-human macrophage antibody/TAMRA, SE (apoptotic cell) events. The stimulation of cell uptake by adiponectin was greater than that exhibited by recombinant C1q protein in parallel experiments. This activity was reproduced by other sources of recombinant adiponectin protein, including that produced by *Escherichia coli*– and mammalian cell–produced murine adiponectin (data not shown). Furthermore, adiponectin did not affect the uptake of microbeads opsonized with BSA, IgG, or C3b, suggesting that it is not involved in the regulation of general phagocytic mechanisms. These findings differ from the conclusions of other studies reporting that adiponectin inhibits the phagocytic actions of macrophages toward microspheres and late apoptotic bodies in vitro (37, 43). One of these studies also reported that adiponectin purified from human plasma will stimulate the phagocytosis of late apoptotic bodies in the presence of LPS in vitro (43). In contrast, our experiments showed that recombinant adiponectin only stimulated the uptake of early, not late, apoptotic bodies and that LPS did not stimulate uptake under either condition (data not shown). This discrepancy may result from differences in adiponectin protein preparations between the 2 studies or possibly from adiponectin binding of LPS (44), which would result in an indirect effect on late apoptotic body uptake through sequestration of this endotoxin.

Because recombinant or purified adiponectin proteins could potentially produce artifactual results in vitro, adiponectin-mediated apoptotic cell uptake was also evaluated in vivo using gain- and loss-of-function genetic manipulations. For these experiments, TAMRA, SE–labeled apoptotic cells were introduced to the peritoneum of thioglycollate-pretreated mice, and macrophages were recovered and assessed for TAMRA, SE positivity by flow cytometric analysis. In these assays, peritoneal macrophages of APN-KO mice displayed reduced uptake of apoptotic cells compared with those of WT mice. Conversely, adenovirus-mediated expression of the adiponectin gene stimulated apoptotic body uptake in both WT and APN-KO mice.

The ability of adiponectin to promote apoptotic cell disposal is likely due to its ability to opsonize apoptotic debris and facilitate its binding to the macrophage cell surface. In this regard, members of the collectin family of proteins, including surfactant proteins A and D, and C1q opsonize apoptotic cells and pathogens via their

globular head regions (26, 35, 45). Like adiponectin, these proteins are expressed at high levels, either systemically or in select mucosal surfaces in lung and gastrointestinal tract which are constantly bombarded by environmental stress. Surfactant proteins and C1q recognize an array of apoptotic cell–associated molecular patterns that serve as "eat-me" markers on dying cells. Because these apoptotic cell recognition motifs are diverse, they are generally recognized by abundant proteins via low-affinity interactions. Here, we show by fluorescence microscopy that adiponectin binds to apoptotic cells in a patchy pattern that appears to decorate blebs on the cell surface. Furthermore, we show by quantitative flow cytometry that there is greater binding of adiponectin to apoptotic cells than viable cells, consistent with the finding that collectin protein receptors are upregulated and redistributed to the cell surface as cells undergo apoptosis (36).

Surfactant proteins and C1q also bind to receptors on phagocytic cells and function as a bridge between the phagocytic cell and the material to be ingested. Calreticulin is expressed on both the phagocyte and the apoptotic cell surface, and it plays an important role in the uptake of apoptotic material through its interactions with CD91 (25, 36). Here, it is shown that both calreticulin and CD91 are involved in adiponectin-mediated uptake of apoptotic cells. The addition of anti-calreticulin or anti-CD91 antibody effectively blocked adiponectin-stimulated phagocytosis in both human macrophages and THP-1 cells. These findings were corroborated by RNA interference methods, in which a reduction in calreticulin or CD91 expression by siRNA resulted in appreciable reductions in adiponectin-stimulated apoptotic cell phagocytosis in THP-1 cells. In contrast, the putative adiponectin receptors did not appear to have a role in this activity. While AdipoR1, AdipoR2, and T-cadherin expression could be detected on the surface of THP-1 cells, reductions in their expression by siRNA methods had no detectable effect on the adiponectin-stimulated uptake of apoptotic cells. Thus, while AdipoR1 and AdipoR2 may mediate the metabolic properties of adiponectin (12), calreticulin controls aspects of adiponectin's antiinflammatory actions.

It is well established that the accumulation of apoptotic debris exacerbates symptoms of inflammation and autoimmunity (26, 46). Thus, to further assess the functional significance of adiponectin-mediated apoptotic cell clearance in vivo, we analyzed adiponectin deficiency and overexpression in the *lpr* strain of mice that display inflammatory phenotypes in the C57BL/6 background. Compared with parental strains, APN-KO/*lpr* mice display a greater degree of systemic inflammation, including higher titers of autoreactive ANA antibodies and a greater degree of lymphadenopathy. Furthermore, unlike the B6.*lpr* mice, APN-KO/*lpr* mice in the C57BL/6 background displayed features of an autoimmune phenotype, including detectable titers of anti-dsDNA antibodies, glomerular tuft volume enlargement, and proteinuria. Consistent with these observations, APN-KO/*lpr* mice had higher frequencies of cell corpses in submandibular lymph nodes and impaired uptake of apoptotic cells in the peritoneum. In contrast with B6.*lpr*, the *lpr* mutation in MRL/Mp$^{+/+}$ background is sufficient to produce autoimmune phenotypes. Adenovirus-mediated overexpression of adiponectin in MRL.*lpr* mice promoted the clearance of apoptotic cells in the peritoneum and markedly diminished the levels of cell corpses that could be detected in histological sections of lymph nodes. Notably, adiponectin overexpression at the 2-week time point diminished both ANA and anti-dsDNA antibody titers, glomerular tuft volume, and levels of urinary albumin. Collectively, the genetic gain- and loss-of-function experiments support the hypothesis that adiponectin functions to promote the clearance of apoptotic debris from the body and that this activity can influence the degree of systemic inflammation. It should also be noted that TNF-α is a key regulator in murine models of autoimmunity (47). Thus, adiponectin can influence the autoimmune phenotype through at least 2 mechanisms involving TNF-α. First, adiponectin can act directly on a variety of cells to suppress TNF-α synthesis (e.g., Shibata et al., ref. 21). In addition, adiponectin-stimulated engulfment of early apoptotic bodies suppresses TNF-α production by macrophages whereas the accumulation engulfment of late apoptotic bodies leads to the production of proinflammatory cytokines (26).

We hypothesize that adiponectin represents one of many functionally redundant proteins involved in apoptotic cell clearance. While our data show that adiponectin deficiency is not sufficient to result in an accumulation of apoptotic cells under nonstress conditions, this phenotype was detected following massive thymocyte apoptosis resulting from dexamethasone treatment or the injection of apoptotic cells into the peritoneal cavity. Similarly, impaired clearance of apoptotic cells associated with adiponectin deficiency was revealed when APN-KO mice were crossed with *lpr* mice. These data indicate that impaired clearance of apoptotic cells due to adiponectin deficiency is observed when apoptotic cells are produced at a higher than normal frequency or there are other deficiencies in the machinery that clears these cells. Furthermore, adiponectin deficiency in itself is not sufficient to produce an autoimmune phenotype, but this phenotype may be achieved when the animal is stressed or crossed into the proper genetic background.

In summary, we demonstrate a mechanistic link between obesity and systemic inflammation by showing that the adipocyte-derived cytokine adiponectin functions to promote the clearance of early apoptotic debris. This activity is mediated by calreticulin expressed on the phagocytic cell surface and not by any of the previously identified adiponectin receptors. Because the accumulation of cell corpses can cause inflammation and immune system dysfunction, these findings suggest what we believe to be a previously undocumented mechanism by which hypoadiponectinemia can contribute to the development of diabetes, atherosclerosis, and other complex diseases in which chronic inflammation is a contributing factor.

Methods

Materials. WT and *lpr* mice on C57BL/6 backgrounds (B6.*lpr*) and *lpr* mice on MRL/Mp$^{+/+}$ (MRL.*lpr*) backgrounds were purchased from The Jackson Laboratory. Adiponectin knockout (APN-KO) mice on a C57BL/6 background were used (8). Jurkat T cells and THP-1 cells were purchased from ATCC. Recombinant human adiponectin from baculovirus-insect cell expression system was obtained from Nosan Corp. Recombinant mouse adiponectin was prepared from *E. coli* as described previously (11). Human C1q protein was purchased from Quidel Corp. Anti-calreticulin antibody (chicken IgY) was purchased from Affinity BioReagents, anti-calreticulin antibodies (goat polyclonal and rabbit polyclonal) were purchased from Santa Cruz Biotechnology Inc. and Upstate USA Inc., and anti-CD91 antibody was purchased from American Diagnostica Inc. MagneHis Protein Purification System was purchased from Promega. Ad–β-gal and Ad-APN were prepared as described previously (11).

Treatment of mice with dexamethasone. All animal experiments were performed according to institutional guidelines and the Institutional Animal Care and Use Committee (IACUC) guidelines. The experimental protocol was approved by Boston University School of Medicine's IACUC and complied with NIH's Guide for the Care and Use of Laboratory Animals. APN-KO and

WT mice were used at 10–12 weeks of age. Dexamethasone sodium phosphate (0.2 mg, Abraxis BioScience) or vehicle was injected i.p. into mice (28). In some experiments, 2×10^8 PFU of Ad-APN or Ad–β-gal was injected into the jugular vein of mice 2 days prior to the injection of dexamethasone. At 24 hours after dexamethasone injection, mice were sacrificed, and a lobe from each thymus was fixed in formalin and embedded in paraffin. Sections were stained with TUNEL (Roche Diagnostics) to detect apoptotic cells and with rat anti-mouse CD11b antibody (GeneTex Inc.) followed by treatment with rhodamine-conjugated secondary antibody to detect macrophages. Quantification of all TUNEL staining and macrophage staining was performed by examining 6 randomly selected high power fields (×400) in each sample. Macrophage phagocytosis of TUNEL-positive apoptotic debris was quantified as described previously (29). In some experiments, sections were stained with anti-mouse adiponectin antibody. This procedure was followed by treatment with Alexa Fluor 488–conjugated secondary antibody before staining with anti-calreticulin antibody followed by treatment with Alexa Fluor 594–conjugated secondary antibody or anti-mouse CD11b antibody followed by treatment with Alexa Fluor 594–conjugated secondary antibody. In some experiments, each thymus section was stained with goat anti-mouse adiponectin antibody (R&D Systems) or goat IgG as a negative control followed by treatment with biotinylated anti-goat IgG. Visualization of immune complexes with streptavidin-HRP and diaminobenzidine was followed by a methyl green counterstain.

Treatment of thymocytes with dexamethasone. Thymocytes were collected from WT mice (8 weeks). Collected thymocytes were preincubated with recombinant adiponectin (50 μg/ml) or vehicle for 1 hour; this was followed by treatment with dexamethasone (1 μM) for 4 hours. Apoptotic cells were detected with TUNEL staining and analyzed by microscopy. Over 200 thymocytes were analyzed per sample.

Apoptotic cell phagocytosis in the peritoneum. WT, APN-KO, and B6.*lpr* mice were used at 10–12 weeks of age, and MRL.*lpr* mice were used at 8 weeks of age. APN-KO/*lpr* mice were used at 10 weeks of age. Inflammatory macrophages were recruited into the peritoneum by injection of thioglycollate. At 3 days after injection, TAMRA, SE–labeled apoptotic Jurkat T cells (1×10^7 cells) were injected into abdomen of mice (48). After 30 minutes, peritoneal cells were collected from the abdominal cavities. To remove erythrocytes and unphagocytosed apoptotic bodies, cells were incubated on polystyrene dishes for 1 hour and washed 3 times gently. After collection, cells were stained with FITC-conjugated anti-mouse F4/80 antibody (AbD Serotec). Macrophage uptake of apoptotic cells was determined by flow cytometric analysis of dual-labeled macrophages. In some experiments, the 2×10^8 PFUs of Ad-APN or Ad–β-gal were injected into the jugular veins of mice at the time of thioglycollate treatment. At 3 days after infection, apoptotic Jurkat T cells were injected into the peritoneal cavity. In some experiments, apoptotic cells were preincubated with recombinant human adiponectin (50 μg) or vehicle for 60 minutes. Inflammatory macrophages recruited to peritoneum were quantified as described previously (46). In brief, 3 days after thioglycollate i.p., cells were recovered by peritoneal lavage with 5 ml PBS. Cells were initially counted on a hemocytometer, and macrophage levels were quantified on cytospins stained with Diff Quik (Dade Behring). TNF-α levels in the lavage fluid were measured with mouse TNF-α ELISA kits (R&D Systems).

Preparation of apoptotic Jurkat T cells and human neutrophils. Early apoptotic Jurkat T cells and early apoptotic neutrophils, which were isolated from peripheral blood by density gradient centrifugation, were produced by UV exposure at 254 nm for 10 minutes, followed by incubation for 2 hours in RPMI/10% FBS. Late apoptotic Jurkat T cells were produced by 10 minutes of UV exposure followed by incubation for 24 hours in RPMI/10% FBS. Apoptosis was detected by annexin V (R&D Systems) binding using flow cytometric analysis. UV exposure followed by 2 hours in RPMI/10% FBS typically led to 60%–70% apoptosis whereas the 24-hour incubation in RPMI/10% FBS led to approximately 90% apoptosis. Early and late apoptotic Jurkat T cells and early apoptotic human neutrophils were also assessed by their ability to exclude trypan blue upon microscopic analysis (typically >95% for early and <30% for late apoptotic cells). Apoptotic or viable Jurkat T cells and early apoptotic human neutrophils were labeled with TAMRA, SE (Invitrogen) (48).

Generation of APN-KO/lpr mice. APN-KO mice and *lpr* mice were interbred to produce homozygous groups of mice with the following genotypes: APN-KO, *lpr*, APN-KO/*lpr*, and WT. In APN-KO mice, the adiponectin gene was replaced with the neomycin-resistance gene (1), and the neomycin-resistance gene was determined by PCR analysis using DNA extracted from tail samples. The adiponectin gene primers (WT) and neomycin-resistance gene primers (neomycin) were as follows: WT, forward, 5′-ATGAAGACCTCCTGGGAGAGT-3′; WT, reverse, 5′-AGGAGCTAGCTCTTTCAGTTG-3′; neomycin, forward, 5′-GCCAAGCTCTTCAGCAATATCACGG-3′; and neomycin, reverse, 5′-ACTGGGCACAACAGACAATCGGC-3′. The *lpr* alleles were detected using 3 primers that produced 180-bp or 560-bp products, respectively. The *lpr* primers were as follows: 5′-AGGTTACAAAAGGTCACCC-3′ and 5′-GATACGAAGATCCTTTCCTGTG-3′ for the WT allele and 5′-CAAACGCAGTCAAATCTGCTC-3′ for the mutated allele.

Analyses of autoimmune phenotype. For these experiments, B6.WT, B6.APN-KO, B6.*lpr*, and B6.APN-KO/*lpr* mice were used at 10, 12, or 20 weeks of age. For some experiments, Ad-APN or Ad–β-gal (4×10^8 PFU) was injected into the subclavicular vein of B6.*lpr* and MRL.*lpr* mice at 10 or 18 weeks of age, respectively. At 14 days after infection, submandibular lymph nodes from each mouse were fixed in formalin and embedded in paraffin. Sections were stained with TUNEL to detect apoptotic bodies. Quantification of all TUNEL staining was performed by examination of 6 randomly selected fields (×200) in each sample. Serum ANA levels were measured by immunofluorescence using Hep2-coated slides (The Binding Site) (29). Serum anti-dsDNA antibody levels were measured by *Crithidia luciliae* dsDNA kit (The Binding Site). Titers were calculated as the inverse of the last positive dilution. Plasma TNF-α levels were measured with mouse TNF-α ELISA kits. Plasma insulin levels were measured with mouse insulin ELISA kits (ALPCO Diagnostics) after 6 hours of fasting. In some experiments, glucose tolerance tests were performed. MRL/*lpr* mice and MRL/$Mp^{+/+}$ mice (WT) were used at 18 weeks of age; mice were injected i.p. with glucose (1 g/kg) after 6 hours of fasting. Blood sugar was quantified with Accu-Check (Roche Diagnostics) at 0, 15, 30, 60 and 120 minutes after glucose injection.

Analysis of renal function and histology. Urine samples were collected using metabolic cages from WT, *lpr*, APN-KO, APN-KO/*lpr*, and MRL.*lpr* mice. Urinary albumin was measured with mouse albumin ELISA quantitation kit (Bethyl Laboratories). Kidneys from each mouse were fixed in formalin and embedded in paraffin. Glomerular cross-sectional areas of at least 25 glomeruli were measured in each animal using computer-assisted pixel counting (Photoshop 7.0; Adobe). Mean glomerular tuft area (A_G) for each animal was calculated from all available glomerular profiles, and tuft volume (V_G) was calculated as well (49) as follows: $V_G = (B/k)(A_G)^{1.5}$, where B is the shape coefficient for an idealized glomerulus ($B = 1.38$) and k is a size distribution coefficient ($k = 1.10$). Immunocomplexes in kidney were detected as described below. Sections were fixed with acetone and stained with FITC-conjugated anti-mouse IgG (Fc specific) F(ab′)2 (Sigma-Aldrich).

In vitro phagocytosis assay. Human mononuclear cells were isolated from peripheral blood by density gradient centrifugation and cultured for 7 days to promote differentiation to macrophages. THP-1 cells were differentiated into macrophages by treatment with phorbol 12-myristate 13-acetate (100 ng/ml) for 3 days. Macrophage phagocytic activity was measured by flow cytometric analysis of dual-labeled cells using a modification of a previously described method (48). TAMRA, SE–labeled (early or late) apoptotic Jurkat T cells (1×10^6 cells) were treated with recombinant adiponectin, human C1q (5 μg/100 μl of RPMI/2% FBS each), or vehicle for 60 minutes and then added to human macrophage or THP-1 cells (1×10^6 cells/500 μl of RPMI/2%

FBS each) for an additional 30 minutes; the final concentration of adiponectin was 10 μg/ml. Under these conditions, the contribution of adiponectin from FBS was estimated to be less than 0.5 μg/ml. Macrophages were washed to remove unphagocytosed apoptotic debris and stained with FITC-conjugated anti-human macrophage antibody (AbD Serotec). Cells were analyzed for rhodamine and FITC labels by flow cytometry (BD). In some experiments, macrophages were preincubated with anti-calreticulin antibody (chicken IgY, 40 μg/ml), nonimmune control IgY (40 μg/ml), anti-CD91 antibody (mouse IgG, 40 μg/ml), or nonimmune control IgG (40 μg/ml) at 37°C for 60 minutes. In some experiments, the phagocytosis assay was performed after stimulation with 0.1 μg/ml of LPS (*E. coli* O55B5; Sigma-Aldrich) for 3 hours. In some experiments, the phagocytosis of apoptotic cells or viable cells was quantified with fluorescent microscopic analysis after washing macrophages. In each sample, 200 macrophages were analyzed. Macrophages were considered to have phagocytosed a TAMRA-conjugated apoptotic body when more than 50% of the fluorescent signal was contained within the body of the macrophage, as previously described (46). Phagocytosis of opsonized carboxylate-coated microbeads was also determined in vitro. For these experiments, 1.0 μm red fluorescent (580/605) FluoSpheres carboxylate-modified microspheres (Invitrogen) was opsonized with BSA, human IgG (Sigma-Aldrich), or human C3b (Complement Technology Inc.) according to the manufacturer's instructions. Each type of opsonized fluorescent microbead (1×10^7 beads) was incubated with recombinant adiponectin (50 μg/ml) or vehicle for 60 minutes. This mixture was then combined with macrophages, diluting the concentration of adiponectin to 10 μg/ml.

Binding of adiponectin to apoptotic and viable cells. Apoptotic Jurkat T cells or viable Jurkat T cells (1×10^5 cells each) were incubated with FITC-conjugated recombinant human FITC-APN prepared with the FluoroTag FITC conjugation kit (Sigma-Aldrich) (5 μg/ml) or FITC-conjugated human serum albumin for 60 minutes. Adiponectin binding to the cell surface was determined by microscopy or flow cytometric analysis (25). Early apoptotic Jurkat T cells or viable Jurkat T cells (1×10^6 cells each) were incubated with each concentration of FITC-conjugated recombinant human FITC-APN for 60 minutes. After washing, fluorescence intensity was measured with fluorescence microplate reader (SpectraMax; Molecular Devices). In some experiments, apoptotic and viable Jurkat T cells were preincubated with calreticulin (200 μg/ml) or control chicken IgY for 60 minutes prior to incubation with 10 μg/ml FITC-APN.

Analysis of adiponectin-calreticulin interactions. The membrane fractions of THP-1 macrophages were isolated by ultracentrifugation. THP-1 macrophages were sonicated and centrifuged at 1,000 *g* for 10 minutes. The supernatant was centrifuged at 100,000 *g* for 60 minutes. The pellet containing the membrane fraction was dissolved in buffer containing 1% Triton X. Membrane fractions were incubated with polyhistidine-tagged adiponectin (10 μg/ml) or vehicle for 2 hours, precipitated with MagneHis particles (Promega), and separated by electrophoresis on denaturing SDS 10% polyacrylamide gels. Proteins were stained with carrier-complexed silver, and the candidate band was excised and digested with trypsin. Tryptic peptides were analyzed by MALDI-MS using a Voyager-DE STR (Applied Biosystems). Peptide mass fingerprints were analyzed with the protein prospector program MS-Fit (University of California, San Francisco, Mass Spectrometry Facility: http://prospector.ucsf.edu/prospector) using the database NCBInr.2005.01.06. In some experiments, the proteins were transferred to membranes, and immunoblot analysis was performed with anti-adiponectin monoclonal antibody (ANOC9135) or anti-calreticulin antibody. In some experiments, membrane fractions were incubated with polyhistidine-tagged mouse adiponectin (10 μg/ml) or vehicle for 60 minutes and immunoprecipitated with anti-calreticulin antibody or nonimmune control IgG (goat). Following transfer to membranes, immunoblot analysis was performed with the indicated antibodies. Analysis of adiponectin binding to cell-surface calreticulin was performed by incubating intact THP-1 macrophages with adiponectin (200 μg/ml) or vehicle for 60 minutes. Cells were treated with anti-calreticulin antibody (chicken IgY, 10 μg/ml) for 60 minutes, stained with FITC-conjugated anti-chicken IgY, and analyzed by flow cytometric analysis. Differentiated THP-1 macrophages were also incubated with different concentrations of FITC-APN for 60 minutes. Data were analyzed by Microsoft Excel 2003 to produce a logarithmic trend line and calculate binding affinity. In some experiments, macrophages were preincubated with calreticulin (200 μg/ml) or control chicken IgY for 60 minutes prior to incubation with 6 μg/ml FITC-APN. Fluorescence intensity was measured with a fluorescence microplate reader. In some experiments, differentiated THP-1 macrophages were incubated with human recombinant adiponectin (5 μg/ml) for 60 minutes. After washing, THP-1 cells were stained with goat anti-human adiponectin antibody (R&D Systems) followed by Alexa Fluor 488–conjugated anti-goat IgG antibody. Then the cells were stained with rabbit anti-calreticulin antibody followed by Alexa Fluor 594–conjugated anti-rabbit IgG antibody.

Analysis of colocalization by microscopy. Fluorescence images were obtained using a Nikon Diaphot fluorescent microscope or a 2-photon laser scanning confocal microscope designed and built in house in collaboration with the lab of Peter So (Massachusetts Institute of Technology, Cambridge, Massachusetts). For the latter experiments, the light source was a frequency-doubled diode laser–pumped titanium-sapphire laser (Coherent). The excitation pulses, approximately 150 fs in duration, 76 MHz repetition rate, were centered at 780 nm. Power was regulated using polarizing optics. Fluorescent light was short-pass filtered at 700 nm and split by 2 extended reflection dichroic mirrors (565 and 500 nm). Long wavelength light passed the 565 nm dichroic mirror and was band-pass filtered from 600 to 660 nm. Intermediate wavelength light, reflected from the 565 nm dichroic mirror and passing the 500 nm dichroic mirror was band-pass filtered from 500 to 550 nm. The short wavelength light reflected from the 500 nm dichroic mirror was band-pass filtered from 435 to 485 nm. All filters and dichroic mirrors were obtained from Chroma Technology Corp. Each channel of fluorescent light was measured by photomultiplier tubes (Hamamatsu Photonics). Images were reconstructed from the point-by-point fluorescence values and processed using ImageJ (http://rsb.info.nih.gov/ij/). To show colocalization, Alexa Fluor 488 and Alexa Fluor 594 signals were merged. Alternatively, when the brightest spots did not overlap, colocalization was assessed by computing the normalized covariance function for the 2 images (50) and showing the relative contribution made at each pixel where the value was positive.

RNA interference in THP-1 cells. siRNA duplexes targeting human adiponectin receptor 1 mRNA, human adiponectin receptor 2 mRNA, human T-cadherin mRNA, and human CD91 mRNA were purchased from QIAGEN, and siRNA duplex-targeting human calreticulin mRNA was purchased from Invitrogen. Differentiated THP-1 macrophages (1×10^6) were transfected for 24 hours with 40 nM siRNA each by lipofectamine 2000 reagent (Invitrogen). Controls were transfected with unrelated siRNA (QIAGEN, Invitrogen). Reductions of cell-surface proteins were analyzed with flow cytometry. Anti-human adiponectin receptor 1 antibody and anti-human adiponectin receptor 2 antibody were purchased from Phoenix Pharmaceuticals Inc. Anti-human T-cadherin was purchased from Santa Cruz Biotechnology Inc. Analysis of phagocytosis of apoptotic bodies with THP-1 macrophages transfected with each siRNA was performed 72 hours after transfection.

Statistics. Data are presented as mean ± SEM. Statistical analysis was performed by a 2-tailed Student's *t* test or ANOVA analysis. A value of $P < 0.05$ was accepted as statistically significant.

Acknowledgments

This work was supported by NIH National Heart, Lung, and Blood Institute grant NO1-HV-28178 and by other grants

from the NIH (AG15052, HL77774, HL86785, and HL81587) to Kenneth Walsh. Yukihiro Takemura was supported by the Uehara Memorial Foundation. Noriyuki Ouchi was supported by an American Heart Association, Northeast Affiliate, Scientist Development grant.

Address correspondence to: Kenneth Walsh, Department of Molecular Cardiology, Whitaker Cardiovascular Institute, Boston University School of Medicine, 715 Albany Street, W611, Boston, Massachusetts 02118, USA. Phone: (617) 414-2392; Fax: (617) 414-2391; E-mail: kxwalsh@bu.edu.

Received for publication July 14, 2006, and accepted in revised form December 5, 2006.

Yukihiro Takemura and Noriyuki Ouchi contributed equally to this work.

1. Weisberg, S.P., et al. 2003. Obesity is associated with macrophage accumulation in adipose tissue. *J. Clin. Invest.* **112**:1796–1808. doi:10.1172/JCI200319246.
2. Ruan, H., and Lodish, H.F. 2004. Regulation of insulin sensitivity by adipose tissue-derived hormones and inflammatory cytokines. *Curr. Opin. Lipidol.* **15**:297–302.
3. Spiegelman, B.M., Choy, L., Hotamisligil, G.S., Graves, R.A., and Tontonoz, P. 1993. Regulation of adipocyte gene expression in differentiation and syndromes of obesity/diabetes. *J. Biol. Chem.* **268**:6823–6826.
4. Maeda, K., et al. 1996. cDNA cloning and expression of a novel adipose specific collagen-like factor, apM1 (AdiPose Most abundant Gene transcript 1). *Biochem. Biophys. Res. Commun.* **221**:286–289.
5. Hu, E., Liang, P., and Spiegelman, B.M. 1996. AdipoQ is a novel adipose-specific gene dysregulated in obesity. *J. Biol. Chem.* **271**:10697–10703.
6. Spranger, J., et al. 2003. Adiponectin and protection against type 2 diabetes mellitus. *Lancet.* **361**:226–228.
7. Yamauchi, T., et al. 2001. The fat-derived hormone adiponectin reverses insulin resistance associated with both lipoatrophy and obesity. *Nat. Med.* **7**:941–946.
8. Maeda, N., et al. 2002. Diet-induced insulin resistance in mice lacking adiponectin/ACRP30. *Nat. Med.* **8**:731–737.
9. Okamoto, Y., et al. 2002. Adiponectin reduces atherosclerosis in apolipoprotein E-deficient mice. *Circulation.* **106**:2767–2770.
10. Shibata, R., et al. 2004. Adiponectin stimulates angiogenesis in response to tissue ischemia through stimulation of amp-activated protein kinase signaling. *J. Biol. Chem.* **279**:28670–28674.
11. Shibata, R., et al. 2004. Adiponectin-mediated modulation of hypertrophic signals in the heart. *Nat. Med.* **10**:1384–1389.
12. Yamauchi, T., et al. 2003. Cloning of adiponectin receptors that mediate antidiabetic metabolic effects. *Nature.* **423**:762–769.
13. Hug, C., et al. 2004. T-cadherin is a receptor for hexameric and high-molecular-weight forms of Acrp30/adiponectin. *Proc. Natl. Acad. Sci. U. S. A.* **101**:10308–10313.
14. Tataranni, P.A., and Ortega, E. 2005. A burning question: does an adipokine-induced activation of the immune system mediate the effect of overnutrition on type 2 diabetes? *Diabetes.* **54**:917–927.
15. Ouchi, N., Kihara, S., Funahashi, T., Matsuzawa, Y., and Walsh, K. 2003. Obesity, adiponectin and vascular inflammatory disease. *Curr. Opin. Lipidol.* **14**:561–566.
16. Ouchi, N., et al. 2003. Reciprocal association of C-reactive protein with adiponectin in blood stream and adipose tissue. *Circulation.* **107**:671–674.
17. Krakoff, J., et al. 2003. Inflammatory markers, adiponectin, and risk of type 2 diabetes in the Pima Indian. *Diabetes Care.* **26**:1745–1751.
18. Matsubara, M., Namioka, K., and Katayose, S. 2003. Decreased plasma adiponectin concentrations in women with low-grade C-reactive protein elevation. *Eur. J. Endocrinol.* **148**:657–662.
19. Engeli, S., et al. 2003. Association between adiponectin and mediators of inflammation in obese women. *Diabetes.* **52**:942–947.
20. Matsushita, K., et al. 2005. Inverse association between adiponectin and C-reactive protein in substantially healthy Japanese men. *Atherosclerosis.* **188**:184–189.
21. Shibata, R., et al. 2005. Adiponectin protects against myocardial ischemia-reperfusion injury through AMPK- and COX-2-dependent mechanisms. *Nat. Med.* **11**:1096–1103.
22. Xu, A., et al. 2003. The fat-derived hormone adiponectin alleviates alcoholic and nonalcoholic fatty liver diseases in mice. *J. Clin. Invest.* **112**:91–100. doi:10.1172/JCI200317797.
23. Ujiie, H., et al. 2006. Identification of amino-terminal region of adiponectin as a physiologically functional domain. *J. Cell. Biochem.* **98**:194–207.
24. Arita, Y., et al. 1999. Paradoxical decrease of an adipose-specific protein, adiponectin, in obesity. *Biochem. Biophys. Res. Commun.* **257**:79–83.
25. Vandivier, R.W., et al. 2002. Role of surfactant proteins A, D, and C1q in the clearance of apoptotic cells in vivo and in vitro: calreticulin and CD91 as a common collectin receptor complex. *J. Immunol.* **169**:3978–3986.
26. Savill, J., Dransfield, I., Gregory, C., and Haslett, C. 2002. A blast from the past: clearance of apoptotic cells regulates immune responses. *Nat. Rev. Immunol.* **2**:965–975.
27. Berg, A.H., and Scherer, P.E. 2005. Adipose tissue, inflammation, and cardiovascular disease. *Circ. Res.* **96**:939–949.
28. Scott, R.S., et al. 2001. Phagocytosis and clearance of apoptotic cells is mediated by MER. *Nature.* **411**:207–211.
29. Aprahamian, T., et al. 2004. Impaired clearance of apoptotic cells promotes synergy between atherogenesis and autoimmune disease. *J. Exp. Med.* **199**:1121–1131.
30. Licht, R., Dieker, J.W., Jacobs, C.W., Tax, W.J., and Berden, J.H. 2004. Decreased phagocytosis of apoptotic cells in diseased SLE mice. *J. Autoimmun.* **22**:139–145.
31. Kelley, V.E., and Roths, J.B. 1985. Interaction of mutant *lpr* gene with background strain influences renal disease. *Clin. Immunol. Immunopathol.* **37**:220–229.
32. Cohen, P.L., and Eisenberg, R.A. 1991. *Lpr* and *gld*: single gene models of systemic autoimmunity and lymphoproliferative disease. *Annu. Rev. Immunol.* **9**:243–269.
33. Morse, H.C., III, et al. 1985. Abnormalities induced by the mutant gene, *lpr*. Patterns of disease and expression of murine leukemia viruses in SJL/J mice homozygous and heterozygous for *lpr*. *J. Exp. Med.* **161**:602–616.
34. Botto, M., et al. 1998. Homozygous C1q deficiency causes glomerulonephritis associated with multiple apoptotic bodies. *Nat. Genet.* **19**:56–59.
35. Ogden, C.A., et al. 2001. C1q and mannose binding lectin engagement of cell surface calreticulin and CD91 initiates macropinocytosis and uptake of apoptotic cells. *J. Exp. Med.* **194**:781–795.
36. Gardai, S.J., et al. 2005. Cell-surface calreticulin initiates clearance of viable or apoptotic cells through trans-activation of LRP on the phagocyte. *Cell.* **123**:321–334.
37. Yokota, T., et al. 2000. Adiponectin, a new member of the family of soluble defense collagens, negatively regulates the growth of myelomonocytic progenitors and the functions of macrophages. *Blood.* **96**:1723–1732.
38. Kumada, M., et al. 2004. Adiponectin specifically increased tissue inhibitor of metalloproteinase-1 through interleukin-10 expression in human macrophages. *Circulation.* **109**:2046–2049.
39. Stern, M., Savill, J., and Haslett, C. 1996. Human monocyte-derived macrophage phagocytosis of senescent eosinophils undergoing apoptosis. Mediation by alpha v beta 3/CD36/thrombospondin recognition mechanism and lack of phlogistic response. *Am. J. Pathol.* **149**:911–921.
40. Voll, R.E., et al. 1997. Immunosuppressive effects of apoptotic cells. *Nature.* **390**:350–351.
41. Newman, S.L., Henson, J.E., and Henson, P.M. 1982. Phagocytosis of senescent neutrophils by human monocyte-derived macrophages and rabbit inflammatory macrophages. *J. Exp. Med.* **156**:430–442.
42. Byrne, A., and Reen, D.J. 2002. Lipopolysaccharide induces rapid production of IL-10 by monocytes in the presence of apoptotic neutrophils. *J. Immunol.* **168**:1968–1977.
43. Saijo, S., et al. 2005. Inhibition by adiponectin of IL-8 production by human macrophages upon coculturing with late apoptotic cells. *Biochem. Biophys. Res. Commun.* **334**:1180–1183.
44. Peake, P.W., Shen, Y., Campbell, L.V., and Charlesworth, J.A. 2006. Human adiponectin binds to bacterial lipopolysaccharide. *Biochem. Biophys. Res. Commun.* **341**:108–115.
45. Wright, J.R. 2005. Immunoregulatory functions of surfactant proteins. *Nat. Rev. Immunol.* **5**:58–68.
46. Potter, P.K., Cortes-Hernandez, J., Quartier, P., Botto, M., and Walport, M.J. 2003. Lupus-prone mice have an abnormal response to thioglycolate and an impaired clearance of apoptotic cells. *J. Immunol.* **170**:3223–3232.
47. Kollias, G. 2005. TNF pathophysiology in murine models of chronic inflammation and autoimmunity. *Semin. Arthritis Rheum.* **34**:3–6.
48. Taylor, P.R., et al. 2000. A hierarchical role for classical pathway complement proteins in the clearance of apoptotic cells in vivo. *J. Exp. Med.* **192**:359–366.
49. Meyer, T.W., and Rennke, H.G. 1988. Increased single-nephron protein excretion after renal ablation in nephrotic rats. *Am. J. Physiol.* **255**:F1243–F1248.
50. Vereb, G., et al. 2000. Cholesterol-dependent clustering of IL-2Ralpha and its colocalization with HLA and CD48 on T lymphoma cells suggest their functional association with lipid rafts. *Proc. Natl. Acad. Sci. U. S. A.* **97**:6013–6018.